Journal of Atmospheric and Solar-Terrestrial Physics 130-131 (2015) 89–95

Contents lists available at ScienceDirect

Journal of Atmospheric and Solar-Terrestrial Physics

journal homepage: www.elsevier.com/locate/jastp

# Lidar observations of cirrus clouds in Buenos Aires

S. Gabriela Lakkis [a,d,*], Mario Lavorato [b,c,f], Pablo Canziani [d,e,f], Hector Lacomi [b,g]

[a] Facultad de Ciencias Agrarias, Pontificia Universidad Catól ica Argentina (UCA), Argentina
[b] División Radar Laser, DEILAP-CITEDEF, Argentina
[c] Grupo TAMA, Universidad Tecnológica Nacional-Facultad Regional de Haedo, (UTN-FRH), Argentina
[d] Unidad de Investigación y Desarrollo de las Ingenierías, Universidad Tecnológica Nacional, Facultad Regional Buenos Aires (UTN-FRBA), Argentina
[e] Consejo Nacional de Investigaciones Científicas y Técnicas (CONICET), Argentina
[f] Facultad de Ciencias Físico-Matemáticas e Ingeniería, Pontificia Universidad Católica Argentina (UCA), Argentina
[g] Grupo SyCE-FRH, Universidad Tecnológica Nacional, Facultad Regional Haedo (UTN-FRH), Argentina

ARTICLE INFO

*Article history:*
Received 3 December 2014
Received in revised form
27 May 2015
Accepted 28 May 2015
Available online 29 May 2015

*Keywords:*
Lidar measurements
Cirrus clouds
Optical depth
Lidar ratio

ABSTRACT

Characterization of cirrus clouds over Buenos Aires (34.6°S, 58.5°W) using a ground based lidar is presented. The study, carried out for the period 2010–2011, reveals that cirrus are usually found in the altitude region 8–11 km, with mid-cloud temperatures values varying between −75 °C and 55 °C. The clouds, whose bases altitudes display significant variability while their tops remains close to the tropopause, show geometrical thickness ranging from 1.2 to 5 km, with on average value 3.0 ± 0.9 km. Most commonly observed cirri can be characterized as optically thin cirrus rather than dense ones, with a mean optical depth value of 0.26 ± 0.11 and an applied multiple scattering factor $\eta$ of 0.85 ± 0.07. In this region, the optical depth increases with increasing geometrical thickness with a partially linear correlation. Lidar ratios are also analyzed and on average the value is 32 ± 17 sr.



## 1. Introduction

High altitude clouds have a major influence on the radiation budget of the Earth-atmosphere system and induce various climate feedbacks which cannot be overlooked (Stephens et al., 1990). In particular, cirrus clouds with large horizontal and vertical extensions play an important role in the Earth's climate system through the albedo effect, reflecting solar radiation while the greenhouse effect traps the long-wave radiation. Additionally, cirrus clouds are important in the stratosphere–troposphere exchange (STE) (Corti et al., 2006) and they have a crucial role interacting with the tropopause layer (Beyerle et al., 1998; Immler, and Schrems, 2002). In spite of the considerable efforts made in the last few years regarding cirrus properties, the parameterization of these ice clouds remains one of the biggest challenges in global climate analysis. Given that cirrus plays an important part in radiative balance and the troposphere–stratosphere exchange a detailed monitoring of their properties at different geographical locations is crucial to understand the climate. Many field experiments to measure cirrus clouds have been conducted by various researchers over a range of latitudes, with different techniques and different study aims: the INCA project concerning cirrus clouds over Punta Arenas, Chile (Immler and Schrems, 2002), Satellite Cloud Climatology Project (ISCCP) (Eleftheratos et al., 2011), the European experiments on cirrus clouds European Cloud Radiation Experiment (EUCREX) (Larsen et al., 1998) to name a few. Lidar remote sensing is a valuable tool for measuring the time and spatial evolution of the atmospheric boundary layers (e.g. planetary boundary layer, tropopause layer) as well as to investigate the physics properties of the particles composing cloud, with the exception of water clouds, because of the capability of the laser beam to point upward into the atmosphere (Wang et al., 2005) and providing range resolved information. Laser remote sensors can provide valuable information of the vertical structure and the composition of the atmosphere at high resolution. In particular, elastic backscatter lidars and ceilometers (low-power backscatter lidars) are very useful in deriving geometrical and optical properties of the clouds, which are essential in understanding the cloud radiation effects both at mid-latitudes and in the tropics. The last two mentioned, both based on the principle of a simple backscatter lidar, can provide cloud parameters through retrieval methods under certain assumptions although ceilometers, fully automatic and operating 24/7, have limitations with the calibration of the lidar signals because of the low signal-to-noise ratio (SNR) (Wiegner and Geiß, 2012). A complete report about the lidar techniques and inter-comparisons can be found in Tapakis and Charalambides (2013) and Wiegner et al. (2014). Studies on high

* Corresponding author at: Facultad de Ciencias Agrarias, Pontificia Universidad Católica Argentina (UCA), Argentina.
*E-mail address:* gabylakkis@uca.edu.ar (S. Gabriela Lakkis).

http://dx.doi.org/10.1016/j.jastp.2015.05.020
1364-6826/

altitude cirrus clouds with information obtained and calculated from lidar observations were carried out for several decades resulting in a wide range of values for their properties. For example, Uthe and Russell (1977) at Kwajalein (8.7°N, 167.7°E) using a ground-based lidar observed cirrus between 12 and 18 km with geometrical thickness of less than 1 km. Giannakaki et al. (2007) using a two-wavelength combined elastic-backscatter Raman lidar located at the Laboratory of Atmospheric Physics in Greece (40.61N, 22.91E) found that cirrus clouds are generally located at heights ranging from 8.6 to 13 km, with mid-cloud temperatures in a range from −65 to −38 °C. Cirrus physical parameters of primary concern are thickness, mean altitude, mid-cloud temperature and lidar ratio since they play an important role in determining cloud radiative properties (Sunilkumar and Parameswaran, 2005). But, it should be noted that the formation of cirrus, its lifetime, vertical and horizontal extend, dynamics, optical and microphysical properties strongly depend on its location and therefore no particular analysis can be considered globally representative of cirrus characteristics. A series of cirrus measurements was conducted in Buenos Aires during 2001–2005 in order to obtain the first comprehensive lidar based cirrus cloud analysis for these latitudes (Lakkis et al., 2009). This contribution showed that at first sight, thick tropopause cirri were found around the ~8–11.5 km height range, with thicknesses in the 2.6–4.2 km range. Although some of the properties of cirrus close to the tropopause over Buenos Aires were described in that study, the ground-based lidar observations provide an excellent opportunity to deepen understanding the geometrical and optical characteristics of the cirrus clouds. With this in mind, a new set of measurement was performed in Buenos Aires from February 2010 to December 2011 using a ground-based lidar located at Villa Martelli, in Buenos Aires province (34.6°S, 58.5°W). The aim in this case is to study the mean characteristics of the cirrus and their short-term temporal variations. The study is organized as follows: in Section 2 a brief description of the lidar system used is presented together with measurements consideration. In Section 3, results are presented in the form of macrophysical and optical properties such as cirrus height, temperature, optical depth and lidar ratio, for the period for the years 2010–2011. Finally, Section 4 provides the summary.

## 2. Experiment system and measurements

The elastic backscatter lidar used is equipped with an Nd:YAG laser (Continuun – Surelite II) having a pulse width of 5 ns at its second harmonic 532 nm wavelength with 350 mJ energy with 10 Hz of pulse rate. A dual telescope receiver system is used to handle the large signal dynamic range (8.2 cm diameter Cassegrain telescope covers the range between 50 m and 6 km, while a 50 cm diameter Newtonian telescope covers from 500 m up to 28 km) with a field of view (FOV) < 1 mrad. The vertical resolution of the elastic signal at 532 nm is equal to 7.5 m. The lidar system was continuously operating during the period from February 2010 to December 2011 under clear sky and the measurements were restricted by the visibility of the cirrus from the ground and the absence of aerosols or pollutants to guarantee signals with a quite good signal to noise ratio. The complete dataset corresponds to 40,000 profiles where each profile represents an average of 500 laser shots. To avoid specular reflections for normal incidences that can happens when ice crystals are horizontally oriented in the cloud, the lidar beam was tilted 2.5° from zenith.

In order to obtain reliable cloud parameters, the cloud boundaries must be defined. Immler et al. (2008) pointed out that a “clear definition of what should be classified a cirrus cloud is missing to date”. The overlap between the transmitted beam and the field of view of the receiver determines the lowest altitude limit (Parameswaran et al., 2004). Comstock et al. (2002) pointed out that tropical cirrus are generally observed above 9 km. Liu et al. (2008) found that the cloud base height is usually detected above the 6 km over semi-arid areas. In an attempt to unify criteria and to avoid possible and unwanted inclusion of water clouds, here we will consider the more general definition given by the International Coordination group on Laser Atmospheric Studies (ICLAS) (Linch et al., 2002): cirrus clouds derived from lidar measurements are layers of particle above 6 km situated in an air mass with temperature of −25 °C or colder, which in addition, display a large temporal and spatial variability. With that definition in mind, the cirrus mid-cloud height was defined as the geometric center of the cirrus cloud (Sunilkumar and Parameswaran, 2005) while the cirrus top and base heights were estimated following the threshold method developed by Platt et al. (1994). The method has already been described by several authors (Giannakaki et al., 2007; Wang et al., 2013), but a brief summary may be useful here: the cloud-base altitude is defined as that point at which there is an increase at the lidar signal level equals to two times the standard deviation above the background level. The lidar signal is required to increase for at least 5 successive height intervals in order to avoid the impact of noise. Cloud top height can also be determined by calculating the standard deviation of noise above cloud top and moving downward in altitude. Optical parameters of cirrus clouds can be obtained solving the lidar equations. The complete set of equations that govern lidar signals and Rayleigh scattering theory can be found in Del Guasta et al. (1993), Chen et al. (2002) or Parameswaran et al. (2004) just to name a few. But in brief, it is important here to bear in mind that the backscatter coefficient and an effective lidar ratio can be retrieved using both Klett and Fernald formalism, as proposed by Ansmann et al. (1992). The lidar ratio then corresponds to the ratio of the cirrus optical depth to the backscatter coefficient integrated over the cirrus layers and can be considered as the weighted “mean” lidar ratio (Giannakaki et al., 2007). According to Cadet et al. (2005), the lidar ratio can be obtained using this methodology with reasonable accuracy (with uncertainty of the 20% at most) in the case of thin and thick cirrus. The cloud optical depth ($\tau$) is calculated by integrating the particle extinction coefficient within the cloud boundaries.

The meteorological parameters used to determine the tropopause temperature and height as well as the cloud temperature and pressure (height) values were provided by the Argentine Servicio Meteorológico Nacional (SMN) and correspond to radiosonde measurements, launched at the nearby Ezeiza operational weather station and restricted to 00 UTC and 12 UTC when available.

Multiple scattering effects (MS) must be considered when cirrus clouds are analyzed since they are mainly composed of ice crystals. This effect is strongly related to the field of view of the lidar used, density and thickness of the clouds. According to Eloranta (1998) the multiple scattering effect is significant for large optical thickness ($\tau > 1$) or large FOV. On the other hand, several analyzes from Platt (1978) have laid out approaches for quantifying and correcting for the effects of MS and how the correction factor $\eta$ must be performed and they pointed out that multiple scattering is primarily related to the optical depth. According with Chen et al. (2002), the multiple scattering factor can be calculated from:

$$\eta = \frac{\tau}{\exp^{\tau} - 1} \tag{1}$$

The smaller value of $\eta$ the more important the multiple scattering effect is. The latter expression is the one we have used for this study, considering that we are dealing with $\tau < 1$ and FOV < 1 mrad.

## 3. Results and discussion

To ensure reliable cirrus parameters, each cirrus measurement was carried out from at least 30 min up to nine consecutive hours, when the atmospheric conditions were appropriate. Fig. 1 presents the frequency of occurrence of measured cirrus clouds during the analyzed period. The seasonal dependence of these clouds should be analyzed with a higher number of profiles; however from the available data, the frequency of cirrus clouds appears to exhibit an annual pattern with the maximum probability of the observation in the warm months, with an increasing number of clouds during February–June and September–October, and minimum values during September 2010, January 2011 and December 2011. These results are consistent with the values displayed in the International Satellite Cloud Climatology Project (ISCCP) when total amount of diurnal cirrus clouds is consulted and such a seasonal behavior may be related to convection processes from lower to upper troposphere which lead to ice nucleation, as Das et al. (2010) reported. In addition, this season coincides with the period of maximum frequency of severe storms observed in Buenos Aires Province (Canziani et al., 2013)

The distribution of cirrus occurrence with mid-cloud temperature shows that observed cirri population is constrained between −75 °C and −55 °C, with heights generally confined to the 8–14 km, with top and base heights, mean values, around 11.8 and 8.3 km, respectively. Wider ranges of temperature and altitude values were reported in several studies from different latitudes. Sassen and Campbell (2001) have found that the cirrus cloud base (top) altitude are usually located at 8.2 (11.2) km and −34.4 °C (−53.9 °C) from University of Utah while Wang and Sassen (2002) described mid latitude cirrus clouds over Oklahoma with temperature ranged between −40 and −55 °C. Afterwards, Seifert et al. (2007) observed the cirrus over Maldives with a peak appearance around −50 to −70 °C. With larger range and more inclusive values, Das et al. (2010) described cirrus clouds over Taiwan with heights of 8–18 km and temperatures between −30 and −80 °C. Compared with the finding from the above mentioned studies over other latitudes, temperatures and height cirrus clouds values obtained here agree fairly well.

The presence of cirrus clouds is frequently associated with the tropopause layer since their formation process is linked with synoptic scale lifting of air leading to the ice nucleation in low temperature (Das et al., 2010). Remote sensing observations by satellite or lidars (Mather et al., 1998; Wang et al., 1996) have revealed the presence of thin cirrus clouds close to that tropopause layer. The cirrus, generally thin, located in the vicinity of the tropopause play a relevant role in dehydrating the air in the lower stratosphere, as Jensen et al. (1996) reported. Thus, the study of

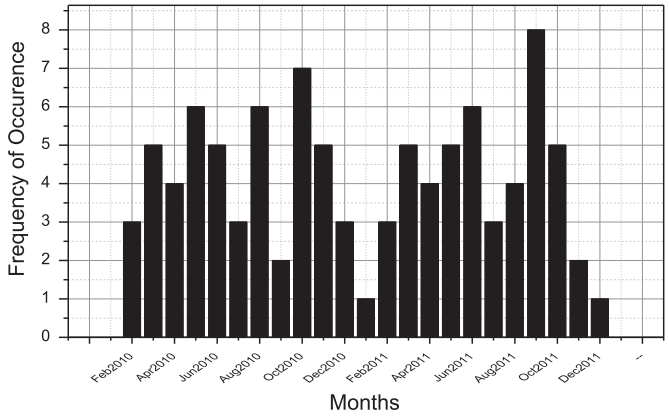


**Fig. 1.** Occurrence of cirrus clouds measured during the period of 2010–2011 over Buenos Aires.

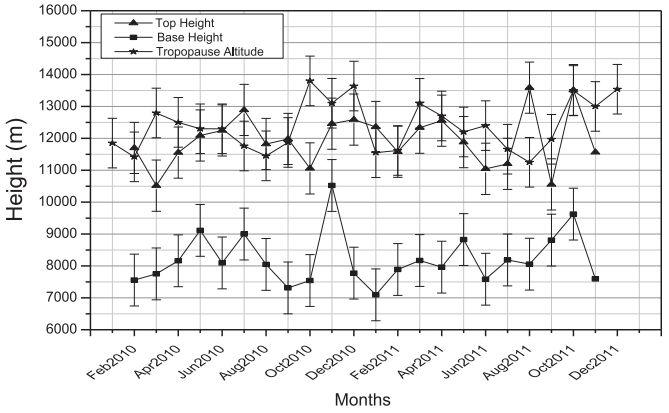


**Fig. 2.** Variations of monthly mean top and base altitudes of cirrus clouds and tropopause altitude. Vertical bars are the standard deviation.

cloud-top and base altitudes with respect to the tropopause altitude is highly relevant. The distance between cloud-top and cloud-bottom altitudes and the tropopause are shown in Fig. 2.

The geometrical parameters of the cirrus were obtained as mean values for the cloud; i.e., average of the parameter determined during the cloud observation.

The tropopause height was obtained following the World Meteorological Organization (WMO, 1957) definition: the lowest level at which the lapse rate decreases to 2 °C/km or less, provided also the averaged lapse rate between this level and all higher levels within 2 km does not exceed 2 °C/km. A perusal of the plot reveals that most cloud-top altitudes are located below but very close to the transition layer, in more than 50% of the observations at less than 1 km from the tropopause; i.e., cirrus clouds are very likely found right under the tropopause. With regard to the cloud base, the observations show that in all the cases the difference between the height of the tropopause and cloud base altitude, is at least larger than 2.5 km. Moreover, the study of cloud-top and bottom altitude with respect to tropopause altitude reveals that most cirrus clouds are contained below the tropopause, although a few of them cross that boundary. Similarly, Sunilkumar et al. (2008) found cirrus clouds located below and very close to the tropical tropopause with few of them with tops penetrating the transition layer and extend into the lower stratosphere.

The macro-physical and optical properties of the cirrus clouds, especially if they are expressed in average values, represent important but slightly incomplete information if temporal and spatial variations are not taken into account. This is due to the fact that water vapor and ice particles concentration vary within the cloud, usually as a non linear process (Keckhut et al., 2013). Within that context, the short term variability of the mean properties is to be considered. Fig. 3 displays the temporal variation of the cloud altitude for 25 May, 2010. As the figure shows the cloud presents a constant descent of the height within the observation period of 9 h: while the altitude of the cloud top remains almost constant with a height of around 12 km, the lower cirrus layer, initially detected close to 9.5 km, extends downward ~1.5 km. The average tropopause altitude on May 2010 was detected close to 12 km, as the Fig. 2 displays. Such displacements of the cloud boundaries have been reported by several authors. Parameswaran et al. (2004) attributed this variation in the cirrus cloud structure to the turbulence existing below the cloud that governs the cloud shape while Nair et al. (2012) considered that these ascending (descendent) movements of cirrus clouds might have been the result not only of upper tropospheric updraft but also due to atmospheric waves.

The previous example is a typical case of observed dense and highly structured cirrus which are usually found close to the

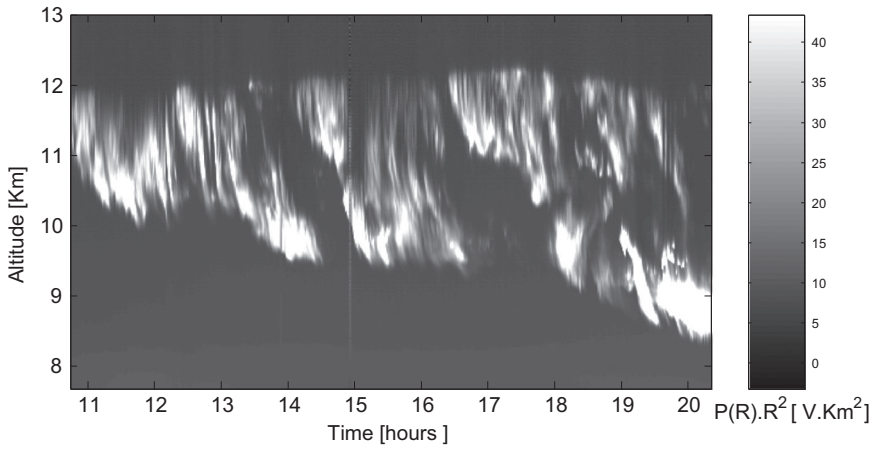


**Fig. 3.** Time series of the altitude detected for the cirrus cloud observed on 25 May, 2010. Note that while the altitude of the cloud top remains almost constant with a height of around 12 km, the cloud bottom experiences a clear descent during the time of observation.

tropopause, according several studies. Most of the cirrus clouds observed in this study persisted throughout the daytime measurement and are dense, while a few of them appeared to be weak and with intermittent presence. These latter are commonly named laminar or single layer thin cirrus (Sunilkumar et al., 2008). The cloud thickness also experiences a temporal variation reaching 3.5 km from the starting thickness of 2.5 km which is to be expected, considering the cloud bottom variations noted above. When considering the whole sample, the geometrical thickness spreads from 1.2 to 5 km, with an average value around $3.0 \pm 0.9$ km. Results derived from different analyzes at mid-latitudes show that mean thicknesses can vary across a wide spectrum of values. In Thessaloniki, Greece, Giannakaki et al. (2007) reported cloud thickness ranging from 1 to 5 km with mean value of $2.7 \pm 0.9$ km, while in China, Wang et al. (2013) observed thickness confined to a range of 0.8–4 km, with an average value of $2.0 \pm 0.6$ km. Compared with the results obtained for mid latitude regions, the mean thickness value over Buenos Aires falls within the reported range. On the other hand Das et al. (2010) found in Taiwan geometrical thickness ranging from 0.24 to 6.65 km with a strong anti-correlation between thickness and cirrus altitude. A similar trend can be found here if the geometrical thickness is plotted as function of the altitude (Fig. 4). Note that Fig. 4 displays thickness, represented at interval of 0.5 km, as function of the base height of cirrus since the cloud base displayed a higher variability as previously mentioned (similar trend can be found if the altitude corresponds to mid cloud altitude). The geometrical thickness remains almost steady for cirrus base altitude $< 9$ km, followed by a rapid decrease for cirrus base altitude $> 9$ km. The negative correlation between both variables, particularly strong from 9 km upward, shows that geometrical thickness decreases as the base height of the cirrus (or mid-cloud height) increases, which implies that cirrus close to the tropopause layer appear to be thin, confirming the results obtained by Sunilkumar and Parameswaran (2005). According to different researches the presence of cirrus with high altitude and low thickness could be linked to convective processes (Canziani et al., 2013).

The optical depth (Fig. 5), also displays a large variability during 25 May, 2010, with increasing values up to 0.4 in the first hours of the morning and in the late afternoon with decreasing values between 12 a.m. and 6 p.m. Maximum and minimum values registered are 0.43 and 0.06 respectively. The example is highly representative of the observations. Sassen and Cho (1992) suggested that the cirrus can be classified as sub-visual cirrus with OD $< 0.03$, thin cirrus with $0.03 < \tau < 0.3$ and dense cirrus with $\tau > 0.3$. With an average value of

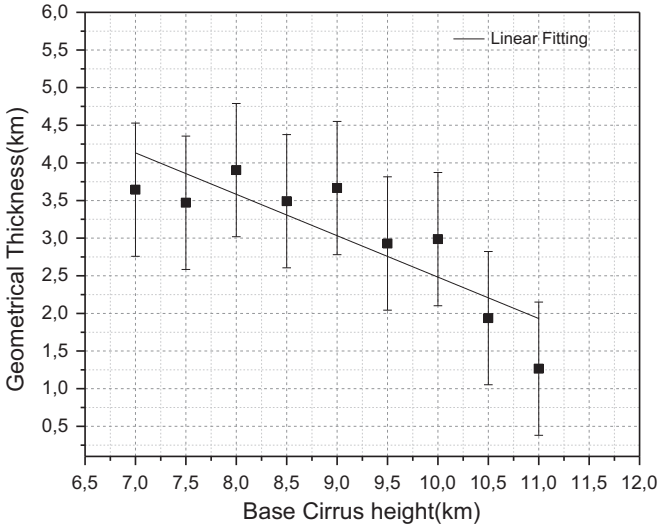


**Fig. 4.** Scatter plot of thickness as function of altitude base cirrus grouped in 0.5 km intervals. Vertical bars are the standard deviation from the mean value.

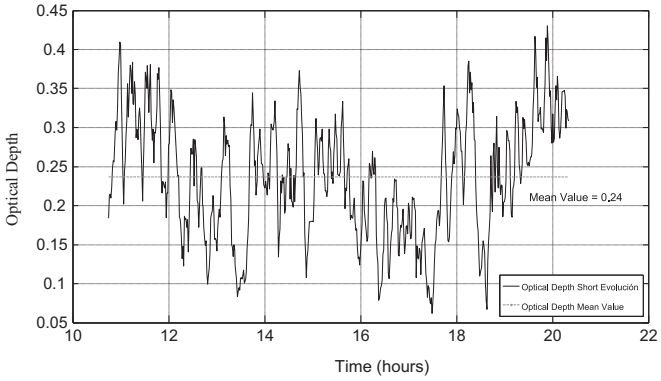


**Fig. 5.** Temporal variations of the optical depth on 25 May, 2010, showing increasing values up to 0.4 in the first hours of the morning and decreasing values in the late afternoon.

$\tau$ below 0.3 on May 25, 2010 the cirrus observed was optically thin, but considering the short time variations the cloud changes from a thin categorization to dense in the first hours of the morning and in the late afternoon. The variability in optical depth depends on the nature of the composition and thickness of the clouds. It is a function of three basic values: the cloud thickness, the number density of the

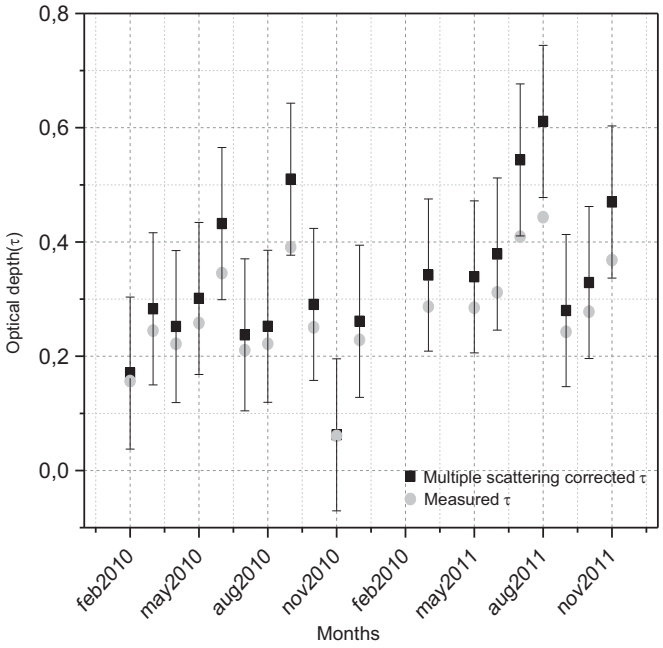


**Fig. 6.** Mean optical depth (measured and multiple scattering corrected) values for the period 2010–2011. Vertical bars are the standard deviation from the mean value.

**Table 1**
Percentage of cirrus classified into different categories.

| Cirrus category | $\tau$ (%) | Corrected $\tau$ (%) |
|---|---|---|
| Sub-visual | – | – |
| Thin | 57.9 | 68.4 |
| Dense | 42.1 | 31.6 |

particles and the mean particle size (Immler and Schrems, 2002; Platt and Harshavardhan, 1988). If the whole sample during the 24 months is considered, more than 65% of the cirrus over Buenos Aires can be classified as thin cirrus and the remaining clouds as dense (Fig. 6 and Table 1), with the lower limit of applied $\eta$ equal to 0.60. In accordance with Giannakaki et al. (2007) there is an indication that optical depth increases with increasing mid-cloud temperature. On the other hand, results for China reported by Wang et al. (2013) showed that the optical depth tends to increase when the cirrus clouds are found in the height range between 5 and 10 km, but when the cloud height increase to 10–13 km range, the $\tau$ decrease with mean values less or equal 0.3. In order to analyze this trend, Fig. 7 shows the dependence of cirrus cloud optical depth on mid-cloud altitude. Note that the optical depth is higher when the cirrus clouds are found in the height range between 8 and 10 km and a rapid decrease in cloud optical depth can be detected when the mid-cloud altitude is $>10$ km. The effect of multiple scattering correction on the optical depth becomes significant when the optical depth increases; this implies that in more than 80% of the observed thin cirrus the difference is not significant while for dense cirrus the optical depth displays a difference of about 30–50% higher. The mean value of the applied $\eta$ was $0.85 \pm 0.07$.

The relationship between optical depth and geometrical thickness is presented in Fig. 8. There is an indication that measured and multiple scattering corrected values of $\tau$ increase with increasing geometrical thickness. Seifert et al. (2007) indicated that thinner clouds would lead to lower optical depth. Sassen and Comstock (2001) also suggested that a linear relationship between both variables is found. Even more evident are the values displayed by Wang et al. (2013) where both parameters seems to be

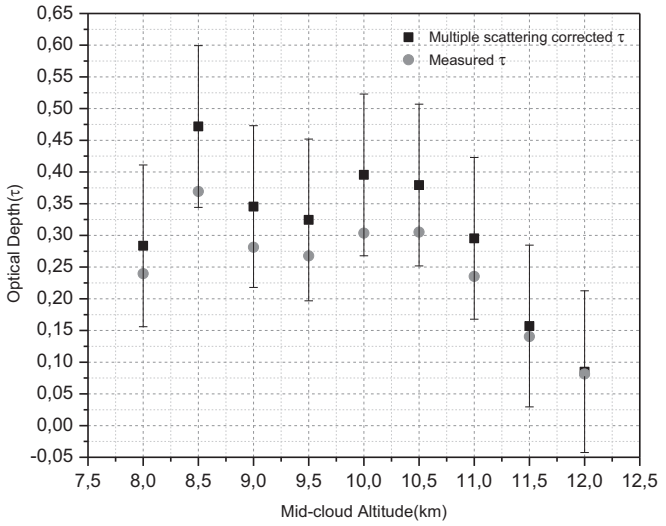


**Fig. 7.** Scatter plot of mean optical depth values with respect to mid cloud heights. Mean value of mid-cloud height is taken for every 0.5 km interval. Standard error is shown with vertical bars.

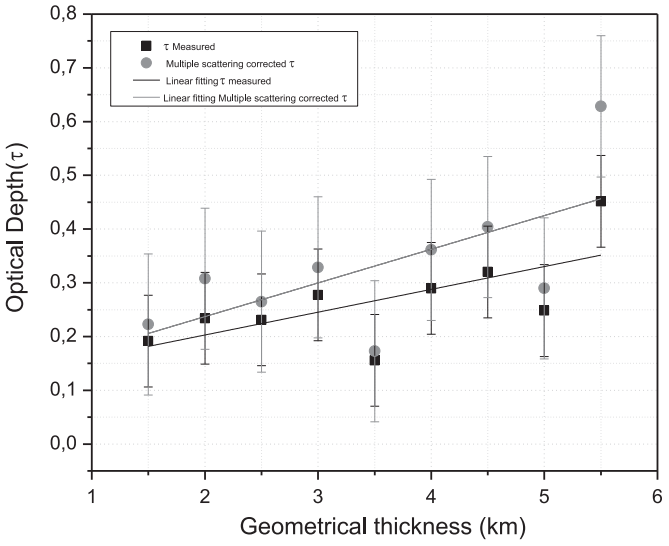


**Fig. 8.** Mean values of optical depth, uncorrected and multiple scattering corrected values, versus geometrical thickness grouped in intervals of 0.5 km. Standard deviations are shown as verticals bars.

in such proportion that doubling the geometrical thickness almost results in doubling the optical depth. However, the correlation found in the above mentioned analysis is higher than the one for our results. Fig. 8 shows that for geometrical thickness values up to 3 km, the relationship is linear but geometrically thicker cirrus clouds seem to have lower mean $\tau$ and in consequence lower mean extinction coefficients. This may be related with cloud-free gaps inside the cirrus or with less and (or) smaller mean size crystals inside the clouds.

Returning to our example on May 25, 2010, within the cloud the lidar ratio also displays a spatial and temporal changing pattern, with measured values spreading through the 20–43 sr range. According to different studies, the lidar ratio can vary within a wide range of values depending on the properties of ice crystals and with height with no clear tendency (Chen et al., 2002). Over the Andros Islands, the lidar ratios were mostly in the range from 10–40 sr, with mean measured values of $20 \pm 8$ sr. Similar lidar ratios were also derived from lidar observations in Taiwan (25°N) presented by Chen et al. (2002). Wang et al. (2013) found lidar

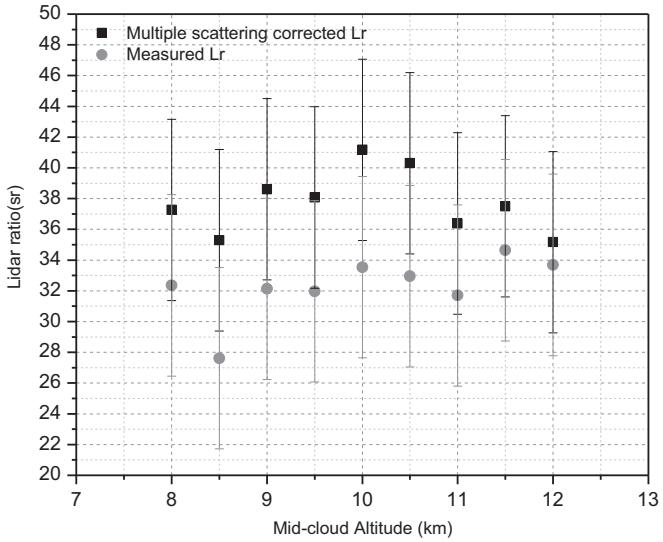


**Fig. 9.** Dependence of lidar ratio (uncorrected and multiple scattering corrected values) on mid-cloud altitude (averaged at 1-km interval).

ratio values varying from 5 to 70 sr and they argued that mean lidar ratio in thin cirrus generally are higher than the opaque ones. Observations over Utah revealed mean values of about 35, 27, 22, 22, and 21 sr for optical depth around 0.12, 0.25, 0.5, 1, 1.2, and 2.5, respectively.

Immler et al. (2008) argued that the reason for the shift in the lidar ratio with latitude is currently unknown. Differences in particle size and shape are possible explanations. Alternatively, a change of the properties of the interstitial aerosol could also have an appreciable influence on the measured optical properties of optically thin ice clouds. Generally, the particles size is known to decrease with altitude. Since cirrus altitude increases with decreasing latitude this trend could explain the change in cirrus lidar ratio. The average measured value on May 25, 2010 was around $28 \pm 15$ sr which is in line with above reported values; this value reaches $32 \pm 17$ sr if we consider the complete dataset. Statistically the obtained values are in good agreement with earlier studies of cirrus. The dependence of the cirrus lidar ratio -mean values- on mid-cloud altitude is shown in Fig. 9. There is no clear interdependence between both variables although it is possible to distinguish two maximum values corresponding to heights around 10 km. Previous and subsequent values of Lr are smaller, and thus 10 km might be considered as a turning point but, nonetheless this trend should be supported with further detailed analysis.

## 4. Summary

Optical properties of cirrus clouds observed using a ground-based lidar at Buenos Aires during 2010–2011 have been analyzed. The sample shows cirrus cloud heights ranging from 8 to 14 km where the temperature is between $-75\,^{\circ}C$ and $-55\,^{\circ}C$. The maximum frequency of occurrence appears to be related with warm months whereas minimum occurrence is found during the austral winter. With the exception of a few cirri with the cloud-tops above the tropopause, most of them are found below the tropopause, with their tops located just below and close to the transition layer.

On average, the geometrical thickness is $3.0 \pm 0.9$ km, though the cirrus bottom displays a significant daily variability during the lidar measurement. A strong anti-correlation between thickness and cirrus altitude is found. Considering the short term variations, the optical depth exhibits a pronounced variability but on average most of the cirrus are thin, according to the classification proposed by Sassen and Cho (1992). Hence the scattering correction becomes significant only in 20% of the sample with mean value close to 0.85.

Measured and multiple scattering corrected $\tau$ values show that for geometrical thickness values up to 3 km the relationship is linear but geometrically thicker cirrus clouds seem to have lower mean $\tau$. This may be related with the size and distribution of the crystals inside the cloud. The lidar ratio values vary in the whole sample from 28 to 39 sr, with a mean value around $32.7 \pm 17.0$ sr, which statistically is in good agreement with earlier cirrus studies.

## Acknowledgments

The authors wish to thank the Pontificia Universidad Católica, Facultad de Ciencias Agrarias, the ANPCyT PICT2012 2927, the Centro de Investigaciones Tecnológicas para la Defensa (CITEDEF) for Lidar System support and also to the Ministerio de Ciencia y Tecnología (MinCyT) PICT03/14240 BID1728OC/AR.

## References

Ansmann, A., Wandinger, U., Riebesell, M., Weitkamp, C., Michaelis, W., 1992. Independent measurement of extinction and backscatter profiles in cirrus clouds by using a combined Raman elastic-backscatter lidar. Appl. Opt. 31, 7113–7131.
Beyerle, J., Schäfer, H.–J., Neuber, R., Schrems, O., Macdemid, I.S., 1998. Dual wavelength lidar observation of tropical high-altitude cirrus clouds during the ALBATROSS 1996 campaign. Geophys. Res. Lett. 25, 919–922.
Cadet, B., Giraud, V., Haeffelin, M., Keckhut, P., Rechou, A., Baldy, S., 2005. Improved retrievals of the optical properties of cirrus clouds by a combination of lidar methods. Appl. Opt. 44, 1726–1734.
Canziani, Osvaldo F., Canziani, Pablo O., Fernandez, Cirelli Alicia, Codignotto, Jorge O, Gimenez, Juan C., Giraut, Miguel A., y Volpedo, Alejandra V., 2013. Aportes Para Abordar la Adaptación al Cambio Climático en la Bahía Samborombón. Boletín técnico de la Fundación Vida Silvestre, Buenos Aires, Argentina.
Chen, W.-N., Chiang, C.-W., Nee, J.-B., 2002. Lidar ratio and depolarization ratio for cirrus clouds. Appl. Opt. 41, 6470–6476.
Comstock, J.M., Ackerman, T.P., Mace, G.G., 2002. Ground-based lidar and radar remote sensing of tropical cirrus clouds at Nauru island: cloud statistics and radiative impacts. J. Geophys. Res. 107, 4714–4727.
Corti, T., Luo, B.P., Fu, Q., Vomel, H., Peter, T., 2006. The impact of cirrus clouds on tropicaltroposphere-to-stratosphere transport. Atmos. Chem. Phys. 6, 2539–2547.
Das, S.K., Nee, J.B., Chiang, C.W., 2010. A LiDAR study of the effective size of cirrus ice crystals over Chung-Li, Taiwan. J. Atmos. Terr. Phys. 72 (9–10), 781–788. http://dx.doi.org/10.1016/j.jastp.2010.03.024.
Del Guasta, M., Morandi, M., Stefanutti, L., Brechet, J., Piquad, J., 1993. One year of cloud LIDAR data from Dumont d'Urville (Antarctica) 1. General overview of geometrical and optical properties. J. Geophys. Res. 98 (D10), 18,575–18,587.
Eleftheratos, K., Zerefos, C.S., Varotsos, C., Kapsomenakis, I., 2011. Interannual variability of cirrus clouds in the tropics in El Niño Southern Oscillation (ENSO) regions based on International Satellite Cloud Climatology Project (ISCCP) satellite data. Int. J. Remote Sens. 32 (21), 6395–6405.
Eloranta, E.W., 1998. Practical model for the calculation of multiply scattered lidar returns. Appl. Opt. 37 (12), 2464–2472.
Giannakaki, E., Balis, D.S., Amiridis, V., Kazadzis, S., 2007. Optical and geometrical characteristics of cirrus clouds over a Southern European lidar station. Atmos. Chem. Phys. 7, 5519–5530. http://dx.doi.org/10.5194/acp-7-5519-2007.
Immler, F., Schrems, O., 2002. Lidar measurements of cirrus clouds in the northern and southern midlatitudes during INCA (55°N, 53°S): a comparative study. Geophys. Res. Lett. 29 (16), 1809. http://dx.doi.org/10.1029/2002GL015077.
Immler, F., Treffeisen, R., Engelbart, D., Krüger, K., Schrems, O., 2008. Cirrus, contrails and ice supersaturated regions in high pressure systems at northern mid latitudes. Atmos. Chem. Phys. 8, 1689–1699.
Jensen, E.J., Owen, B.T., Selkirk, H.B., Spinhirne, J.D., Scheberl, M.R., 1996. On the formation and persistence of subvisible cirrus clouds near the tropical tropopause. J. Geophys. Res. 101, 361–375.
Keckhut, P., Perrin, J.-M., Thuillier, G., Hoareau, C., Porteneuve, J., Montoux, N., 2013. Subgrid-scale cirrus observed by lidar at mid-latitude: variability of the cloud optical depth. J. Appl. Remote Sens. 7 (1), 073530.
Lakkis, S.G., Lavorato, M., Canziani, Pablo Osvaldo, 2009. Monitoring cirrus clouds with lidar in the Southern Hemisphere: a local study over Buenos Aires. 1. Tropopause heights. Atmos. Res. 92 (2009), 18–26. http://dx.doi.org/10.1016/j.atmosres.2008.08.003.
Larsen, H., Gayet, Jean-François, Febvre, G., Chepfer, H., Brogniez, G., 1998. Measurement errors in cirrus cloud microphysical properties. Ann. Geophys. 16 (2),

266–276, European Geosciences Union, (EGU).
Linch, D.K., Sassen, K., Starr, O.'C., Stephens, G., 2002. Cirrus. University Press, Oxford.
Liu, D., Wang, Z., Liu, Z., Winker, D., Trepte, C., 2008. A height resolved global view of dust aerosols from the first year CALIPSO lidar measurements. J. Geophys. Res. 113, D16214. http://dx.doi.org/10.1029/2007JD009776.
Mather, J.H., Ackerman, T.P., Clements, W.E., Barnes, F.J., Ivey, M.D., Hatfield, L.D., Reynolds, R.M., 1998. An atmospheric radiation and cloud station in the tropical western Pacific. Bull. Am. Meteorol. Soc. 79, 627–642.
Nair, A.K.M., Rajeev, K., Mishra, M.K., Thampi, B.V., Parameswaran, K., 2012. Multiyear lidar observations of the descending nature of tropical cirrus clouds. J. Geophys. Res. 117, D18201. http://dx.doi.org/10.1029/2011JD017406.
Parameswaran, K., Sunilkumar, S.V., Krishna Murthy, B.V., Satheeshan, K., 2004. Lidar observations of high altitude cirrus clouds near the tropical tropopause. Adv. Space Res. 34, 845–850. http://dx.doi.org/10.1016/j.asr.2003.08.064.
Platt, C. M. R., et al., 1994. The experimental cloud lidar pilot study (ECLIPS) for the cloud-radiation research, Bull. Am. Meteorol. Soc. 75, 1635–1654.
Platt, C.M.R., Harshvardhan, 1988. Temperature dependencies of cirrus extinction: implications for climate feedback. J. Geophys. Res. 93, 11 051–11 058.
Platt, C.M.R., 1978. Lidar backscatter from horizontal ice crystal plates. J. Appl. Meteorol. 17, 482–488.
Sassen, K., Cho, B.Y., 1992. Subvisual-thin cirrus lidar dataset for satellite verification and climatological research. J. Appl. Meteorol. 31, 1275–1285.
Sassen, K., Campbell, J.R., 2001. A midlatitude cirrus cloud climatology from the facility for atmospheric remote sensing. Part I: macrophysical and synoptic properties. J. Atmos. Sci. 58, 481–496.
Sassen, K., Comstock, J.M., 2001. A midlatitude cirrus cloud climatology from the Facility for Atmospheric Remote Sensing. Part III: Radiative properties. J. Atmos. Sci., 58, 2113–2127.
Seifert, P., Ansmann, A., Müller, D., Wandinger, U., Althausen, D., Heymsfield, A.J., Massie, S.T., Schmitt, C., 2007. Cirrus optical properties observed with lidar, radiosonde, and satellite over the tropical Indian Ocean during the aerosol-polluted northeast and clean maritime southwest monsoon. J. Geophys. Res. 112, D17205. http://dx.doi.org/10.1029/2006JD008352.
Stephens, G.L., Tsay, S.C., Stackhouse, P.W., Flatau, P.J., 1990. The relevance of the microphysical and radiative properties of cirrus clouds to climate and climate feedback. J. Atmos. Sci. 47, 1742–1753.
Sunilkumar, S.V., Parameswaran, K., 2005. Temperature dependence of tropical cirrus properties and radiative effects. J. Geophys. Res. 110, D13205. http://dx.doi.org/10.1029/2004JD005426.
Sunilkumar, S.V., Parameswaran, K., Thampi, Bijoy V., 2008. Interdependence of tropical cirrus properties and their variability. Ann. Geophys. 26, 413–429. http://dx.doi.org/10.5194/angeo-26-413-2008.
Tapakis, R., Charalambides, A.G., 2013. Equipment and methodologies for cloud detection and classification: a review. Sol. Energy 95, 392–430 2013..
Uthe, E.E., Russell, P.B., 1977. Lidar observations of tropical high-altitude cirrus clouds. In: Proceedings of Radiative Conference. International Assocation Meteorology and Atmospheric Physics, Boulder, Colorado, pp. 242–244.
Wang, P.H., Minnis, P., McCormick, M.P., Kent, G.S., Skeens, K.M., 1996. A 6-year climatology of cloud occurrence frequency from stratospheric aerosol and gas experiment II observations (1985–1990). J. Geophys. Res. 101, 29407–29429. http://dx.doi.org/10.1029/96JD01780.
Wang, Jin, Zhang, Lei, Huang, Jianping, Cao, Xianjie, Liu, Ruijin, Zhou, Bi, Wang, Hongbin, 2013. Macrophysical and optical properties of mid-latitude cirrus clouds over a semi-arid area observed by micro-pulse lidar. J. Quant. Spectrosc. Radiat. Transf. 122, 3–12.
Wang, X., Boselli, A., Avino, L.D., Velotta, R., Spinelli, N., Bruscaglioni, P., Ismaelli, A., Zaccanti, G., 2005. An algorithm to determine cirrus properties from analysis of multiple-scattering influence on lidar signals. Appl. Phys. B 80, 609–615.
Wang, Z., Sassen, K., 2002. Cirrus cloud microphysical property retrieval using lidar and radar measurements: II. Midlatitude cirrus microphysical and radiative properties. J. Atmos. Sci. 59, 2291–2302.
Wiegner, M., Geiß, A., 2012. Aerosol profiling with the Jenoptik ceilometer CHM15kx. Atmos. Meas. Tech. 5, 1953–1964. http://dx.doi.org/10.5194/amt-5-1953-2012.
Wiegner, M., Madonna, F., Binietoglou, I., Forkel, R., Gasteiger, J., Geiß, A., Pappalardo, G., Schäfer, K., Thomas, W., 2014. What is the benefit of ceilometers for aerosol remote sensing? An answer from EARLINET. Atmos. Meas. Tech. 7, 1979–1997. http://dx.doi.org/10.5194/amt-7-1979-2014.
WMO, 1957. Definition of the tropopause. WMO Bull. 6, 136.